Distances between DNA and ATP Binding Sites in the TyrR−DNA Complex†

William H. Sawyer,*,‡ Robert Y. S. Chan,‡ John F. Eccleston,§ Barrie E. Davidson,‡ Saiffudin A. Samat,‡ and Yuling Yan||

The Russell Grimwade School of Biochemistry and Molecular Biology, University of Melbourne, Parkville, Australia 3052, The National Institute for Medical Research, Mill Hill, London NW7 1AA, United Kingdom, and Department of Cell Biology, Max Planck Institute for Biochemistry, 82152 Martinsried bei Munchen, Germany

Received January 12, 2000

ABSTRACT: The *Escherichia coli* regulatory protein TyrR controls the expression of eight transcription units that encode proteins involved in the biosynthesis and transport of aromatic amino acids. It binds to DNA as a homodimer with a subunit molecular mass of 57 640 Da, each of which has a single site for the binding of ATP within a central structural domain. This paper reports distances between four sites on the DNA and the ATP binding site as determined by fluorescence resonance energy transfer. The DNA was a 30mer containing a centrally located binding site for TyrR. Replacement of a thymidine residue with an aminouridine residue at positions −9, −7, −3, and 2 of the palindromic oligonucleotide sequence enabled the placement of a single fluorescein group along the major groove of the DNA. The energy transfer acceptor was ATP labeled with a rhodamine group through positions 2′ and 3′ of the ribose, positions that are known to cause minimal interference with the binding of ATP to protein. The dissociation constant for the binding of rhodamine-ATP to TyrR was 300 nM as determined by steady-state fluorescence anisotropy titrations. The energy transfer efficiencies were determined by measuring the level of quenching of donor fluorescence on binding rhodamine-ATP to the TyrR−DNA complex. The experimental transfer efficiencies were compared to theoretical values calculated for a model of the DNA−TyrR complex in which the position of the ATP binding site was allowed to vary over the surface of the monomer unit. Theory was written to account for the transfer from one donor to two acceptors, one on each monomer unit of the TyrR dimer. The results indicate that the ATP binding site is about 40−45 Å from the nearest point on the DNA and distant from the DNA helix−turn−helix binding domain. The effects of ATP binding of (i) increasing the TyrR binding affinity by a factor of 4−5 and (ii) permitting the binding of the tyrosine corepressor must therefore occur because of a significant allosteric change in the conformation of the protein.

The TyrR regulatory protein from *Escherichia coli* controls the expression of at least eight unlinked operons comprising the TyrR regulon whose genes encode enzymes involved in the synthesis and transport of the aromatic amino acids (*1*, *2*). TyrR has a subunit molecular mass of 57 640 Da and exists as a homodimer in solution (*3*). It binds 1 mol of ATP per mole of subunit with half-maximal saturation at 5−7 μM ATP (*4*). Limited proteolysis experiments indicate that the protein consists of three domains (*5*). An N-terminal domain controls transcriptional activation (*6*, *7*) which is modulated by the binding of aromatic amino acids to an ATP-independent site within this domain (*1*, *8*; T. Kwok, J. Rood, and B. E. Davidson, manuscript in preparation). A central domain contains a putative ATP binding site identified on the basis of sequence homology with the ATP binding sites of adenylate kinase and other prokaryotic regulatory proteins that bind ATP, such as NtrC, NifA and XylR (*9*-*10*). The central domain is also thought to contain an ATP-dependent binding site for tyrosine. The C-terminal domain is predicted to form a helix-turn-helix motif (*1*) similar to that found in other DNA binding proteins such as the catabolite activator protein, the *lac* repressor, and lambda *cro*.

TyrR binds to DNA sequences known as TyrR boxes that are characterized by the palindromic consensus sequence $TGTAAAN_6TTTACA$. Two types of TyrR boxes have been recognized (*1*). Strong boxes have more than 10 bp in common with the consensus sequence and bind TyrR in vitro in the absence of an aromatic amino acid coeffector. The affinity of TyrR for strong boxes is enhanced 3−5-fold by the presence of ATP (*1*, *11*, *12*). Weak boxes have a lower level of identity with the consensus sequence and bind TyrR only in the presence of an aromatic amino acid coeffector and when there is an adjacent strong box.

The current view of transcriptional regulation in the TyrR regulon in vivo is that strong boxes are permanently occupied by TyrR dimer−ATP complexes (*6*). The observation that tyrosine induces the self-association of TyrR from a dimer to a hexamer (*6*) has led to the suggestion that in the presence of tyrosine adjacent weak boxes can occupy another binding site on the hexamer, so accounting for the DNase protection of weak boxes under these conditions. The model also

† Supported by grants from the Australian Research Council.

* To whom correspondence should be addressed. Telephone: +61 3 9344 5923. Fax: +61 3 9347 7730. E-mail: w.sawyer@biochemistry.unimelb.edu.au.

‡ University of Melbourne.

§ The National Institute of Medical Research.

|| Max Planck Institute for Biochemistry.

10.1021/bi0000723 CCC: $19.00
Published on Web 04/21/2000

accounts for the loss of transcriptional activity and the DNase protection of weak boxes when bases are inserted between strong and weak boxes of the *tyrP* operon in any number other than that which provides for a full turn of the DNA helix (*13*, *14*).

Particular bases within the TyrR boxes that are involved in close contact with the TyrR protein have been identified by mutation analysis, by methylation, uracil, and ethylation interference experiments (*15*, *16*), and by fluorescence footprinting analysis (*17*). However, further structural studies have been frustrated by the absence of crystals of the TyrR protein (or of the TyrR−DNA complex) that are suitable for X-ray analysis. Low-resolution features of a structure can be obtained through the application of fluorescence resonance energy transfer (FRET), a "spectroscopic ruler" that measures distances within macromolecules and macromolecular complexes (for reviews, see refs *18* and *19*). Fluorescence resonance transfer occurs via an induced dipole interaction that depends on the inverse sixth power of the distance between the donor and acceptor. It has been applied extensively to protein systems, but rarely to the measurement of distances in protein−DNA complexes, probably because of the difficulty of conjugating a fluorescence probe at the optimal position within a DNA sequence. Heyduk and Lee (*20*) assessed FRET between two tryptophan residues in the cAMP receptor protein and terminal sites on fragments of the lac promotor to show that the DNA bending induced by the binding of the protein to DNA was symmetrical. Furey et al. (*21*) measured distances between Cys 751 on the Klenow fragment of DNA polymerase and the single-stranded template portion of the template DNA and showed that the latter possessed helical structure.

The ability to label specific bases within a DNA recognition sequence has important advantages. This approach has proved useful for fluorescently footprinting the DNA−protein interaction and for thermodynamic analysis of the interaction in cases where the fluorescence of an intrinsic tryptophan in the protein is not sensitive to the association (*11*, *16*). In this paper, we report the use of FRET to measure the distance between the ATP binding site in the central domain of the TyrR protein and four sites within the DNA of the TyrR strong box. We show that the measurement of four donor−acceptor distances involving four donor-labeled sites on the DNA is sufficient to identify the position of the ATP binding site in the central domain of the TyrR monomer relative to DNA bases. Fluorescein is used as the fluorescent resonance transfer donor and rhodamine-ATP as the acceptor. In the latter case, the rhodamine is conjugated to the 2′ and 3′ positions of the ribose where it is known to have minimal influence on its interaction with protein (*22*). Since the TyrR protein binds to the DNA as a dimer under the experimental conditions that were used, it was necessary to modify the usual Förster relationship to account for the fluorescence resonance energy transfer from one donor (on the DNA) to two acceptors (one rhodamine-ATP molecule on each monomer of the TyrR dimer).

EXPERIMENTAL PROCEDURES

Materials. FITC (isomer I) was from Molecular Probes (Eugene, OR). ATPγS was from Boehringer (Mannheim, Germany). Oligonucleotides were obtained from CyberSyn. All other reagents were of analytical reagent grade.

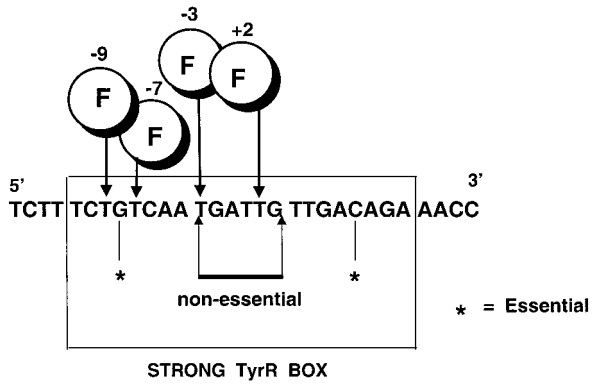

FIGURE 1: Sequence of the 30mer oligonucleotide containing a centrally located TyrR strong box. The arrows indicate the positions where an aminouridine is substituted for a thymidine to permit the conjugation of fluorescein. A circled F indicates a position labeled with fluorescein in separate conjugates. The base positions are numbered relative to the center of the palindromic nucleotide sequence. The asterisks indicate the G and C residues that are absolute requirements for the binding of TyrR. Six nonessential bases are located centrally within the TyrR box.

Oligonucleotide Labeling. The nucleotide sequences of oligonucleotide 30mers containing a centrally located strong box from the *tyrR* operator are shown in Figure 1. Four separate conjugates were prepared, each being labeled with fluorescein at one of four positions. Labeling was accomplished by substituting (aminoethyl)-3-(acrylimido)-2′-deoxyuridine (Glenn Research, Sterling, VA) for a thymidine at positions −9, −7, −3, and 2 in the palindromic oligonucleotide sequence and labeling the free amino group with fluorescein isothiocyanate. These positions correspond to positions 7, 9, 13, and 17 from the 5′ terminus of the 30mer that have been described in a previous publication (*13*). The complementary strand was the unsubstituted complementary sequence. The labeling, HPLC purification, and annealing have been described previously (*11*, *16*, *23*). The annealed duplexes were prepared in 25 mM K_2HPO_4, 100 mM KCl, 1 mM EDTA, 0.1 mM DTT, and 0.02% NaN_3 (buffer F) (*11*, *16*).

TyrR Preparation. TyrR was purified according to published methods using a genetically engineered strain of *E. coli* that overexpresses the protein (*6*, *11*). The preparation was dialyzed against buffer F.

Rhodamine-ATP. The rhodamine-ATP (Figure 2) was synthesized by the reaction of 2′(3′)-*O*-[2-(aminoethyl)-carbamoyl]ATP with lissamine rhodamine sulfonyl chloride as described for the corresponding GTP analogue by Jameson and Eccleston (*21*). We note that although lissamine rhodamine sulfonyl chloride is often described as a pure compound with the sulfonyl chloride in the 4-position of the single aromatic ring, examination of its method of synthesis suggests that it will consist of a mixture of the 2- and 4-sulfonyl chlorides. The NMR spectrum of commercially available material showed the presence of two compounds in equal amounts. Derivatization of the 2′(3′)-*O*-[2-(aminoethyl)carbamoyl]ATP with the 2′-sulfonyl chloride would result in the formation of an analogue which could cyclize to form a nonfluorescent spirosultam (*24*). However, detailed analysis of the product of the reaction by HPLC and absorption spectroscopy showed that although the 2′-sulfonyl chloride derivative was formed during the reaction, in addition to the 4′-derivative, they were cleanly separated from each other by DEAE-cellulose

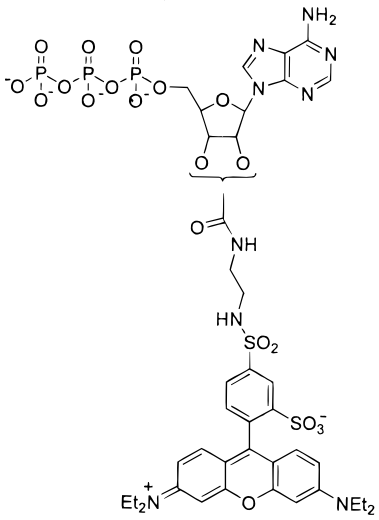

FIGURE 2: Structure of rhodamine-labeled ATP formed by reaction of 2′(3′)-*O*-[2-(aminoethyl)carbamoyl]ATP with lissamine rhodamine chloride.

chromatography, and the material used in this study contained only the fluorescent 4′-derivative.

Quantum Yields. Fluorescence quantum yields (Q) were determined by integration of the area under the emission peak between 480 and 630 nm. Fluorescein in 0.01 M NaOH was used as the standard fluorophore [$Q = 0.93$ (*25*)].

Fluorescence Anisotropy. Fluorescence measurements were taken with a SPEX Fluorolog Tau-2 instrument. Steady-state anisotropy titrations of TyrR with rhodamine-ATP (buffer F) were carried out in 10 mm path length cells at 20 °C. Excitation and emission wavelengths were 560 and 600 nm, respectively. The anisotropy (r) was determined as

$$r = (I_V - I_H)/(I_V + 2GI_H) \quad (1)$$

where I_V and I_H are the vertically and horizontally polarized components of the fluorescence emission, respectively, and G is the grating correction factor.

Fluorescence Energy Transfer. The efficiency of energy transfer (E) was determined by steady-state methods as the quenching of donor emission caused by resonance transfer to the acceptor.

$$E = 1 - Q_{DA}/Q_D \quad (2)$$

where Q_{DA} and Q_D are the quantum yields of the donor in the presence and absence of the acceptor, respectively. For each donor-labeled oligonucleotide, the transfer experiment was conducted in one cuvette in the following sequence: (i) fluorescein-labeled oligonucleotide, (ii) fluorescein-labeled oligonucleotide plus TyrR, and (iii) fluorescein-labeled oligonucleotide, plus TyrR, plus rhodamine-ATP. On the basis of the known binding constants (*6*, *11*), the amount of TyrR added was sufficient to bind all of the fluorescein-labeled DNA present, and the amount of ATP added was sufficient to fully saturate all of the TyrR present. The purpose of this experimental design was to determine changes in the quantum yield of the fluorescein-labeled oligonucleotide due to the binding of TyrR before determining the level of quenching due to energy transfer to the rhodamine-ATP acceptor. Excitation of the fluorescein donor was at 465 nm to minimize sensitization of the rhodamine acceptor by the excitation light. Spectra were corrected for the acceptor excitation at this wavelength using a suitable rhodamine-ATP control. Because of the high concentration of rhodamine-ATP (8.36 μM) required to saturate the site on TyrR, the rhodamine-ATP emission was high despite its low absorption at 465 nm. Thus, the correction required the subtraction of two large numbers, resulting in values with high associated error. For this reason, transfer efficiencies were determined from the donor quench rather than from the acceptor sensitization.

The overlap integral (J) expressing the spectral overlap between the fluorescein emission and the rhodamine absorption was determined as

$$J = \int F_D(\lambda)\epsilon_A(\lambda)\lambda^4 \, \partial\lambda \quad (3)$$

where $\epsilon_A(\lambda)$ is the molar extinction coefficient of the acceptor at wavelength λ and $F_D(\lambda)$ is the fluorescence of the donor normalized on the wavelength scale. The donor−acceptor distance for 50% resonance transfer (R_o) was determined as

$$R_o^6 = (8.79 \times 10^{-25})Q_D\kappa^2 n^{-4} J \quad (4)$$

where Q_D is the quantum yield of the donor and κ^2 is the orientation factor. The refractive index of the intervening medium (n) was assumed to be 1.4. The orientation factor was assumed to be at the dynamic limit where the rates of reorientation of the donor and acceptor are fast compared to the rates of donor emission and transfer. R_o values were determined for each of the labeled DNA−TyrR complexes since the quantum yield of the fluorescein in these complexes depended on the base position that was labeled.

THEORY

The Model. On the basis of our knowledge of the structure of other complexes between DNA and dimeric helix−turn−helix regulatory proteins, we would expect that the 2-fold axis of symmetry of the TyrR dimer would coincide with the 2-fold palindromic symmetry of the operon. The dimer would therefore be formed by the head-to-head association of two monomers as is found in the case of the *cro* and *lac* repressors, and the catabolite gene activator protein (CAP). We therefore consider a simple model in which a dimer, made up of two roughly globular monomer units with radius r (=25 Å), binds to linear DNA as depicted in Figure 3. The radius of 25 Å is based on the volume of an equivalent sphere with a molecular mass equivalent to that of the TyrR monomer. Any point on the surface of the monomer can be defined by the angles θ and ϕ shown in Figure 3. The angle ϕ varies from 0° to 360°, whereas θ varies from 0° to 180°, the θ angles of 181−360° being redundant. The coordinates of a point on the surface of a sphere relative to the center of the sphere are given by

$$x = r \sin\theta \cos\phi$$
$$y = r \cos\theta$$
$$z = r \sin\theta \sin\phi \quad (5)$$

The distance (R_1) from a point on the surface of the left-hand sphere (Figure 3) to a point on the axis of the DNA (x_o,y_o,z_o) is given by

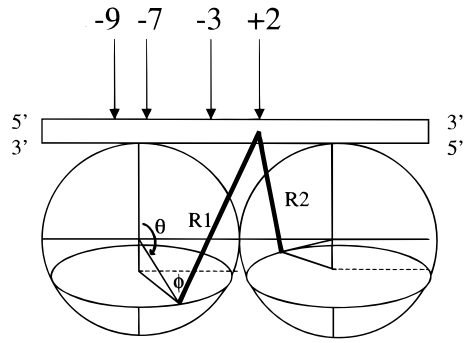

FIGURE 3: Model for the binding of the TyrR dimer to DNA. The diagram is drawn to scale and assumes that the diameter of the TyrR monomer is 50 Å, the DNA helix diameter is 10 Å, and the translation per residue is 3.3 Å. The two TyrR monomers assemble in a head-to-head fashion to bind to the palindromic TyrR strong box. The position of any point on the surface of a monomer can be defined by the angles θ and ϕ. R_1 and R_2 are the distances from the ATP sites on the surface of the monomers to a labeled base on the DNA.

$$R_1 = \sqrt{(x - x_o)^2 + (y - y_o)^2 + (z - z_o)^2} \quad (6)$$

The corresponding distance (R_2) from the reflected point on the second monomer unit to the same point on the DNA is

$$R_2 = \sqrt{(2R - x - x_o)^2 + (y - y_o)^2 + (z - z_o)^2} \quad (7)$$

In the absence of knowledge of the y coordinate position of the label on the oligonucleotide, we have assumed that the florescent donor is located on the central axis of the DNA. This would seem to be a reasonable approximation given that the probe is located in the major groove of the DNA.

Resonance Energy Transfer. The quantum yield of a fluorescent donor (Q_D) in the absence of an acceptor is given by

$$Q_D = \frac{k_D}{k_D + k_{Di}} \quad (8)$$

where k_D is the radiative decay rate and k_{Di} is the radiationless decay rate. However, in the experiments reported here, the acceptor that binds to a single site on each monomer unit in the TyrR dimer is rhodamine-ATP. The transfer is therefore from one donor site on the DNA to two acceptor sites on the TyrR dimer. In the presence of two acceptors, the quantum yield of the donor (Q_{DA}) becomes

$$Q_{DA} = \frac{k_D}{k_D + k_{Di} + k_{T1} + k_{T2}} \quad (9)$$

where k_{T1} and k_{T2} are the rates of energy transfer to acceptors T1 and T2, respectively. The efficiency of transfer [$E = 1 - (Q_{DA}/Q_D)$] is then given by

$$E = \frac{k_{T1} + k_{T2}}{k_D + k_{Di} + k_{T1} + k_{T2}} \quad (10)$$

From Förster theory (for a review, see ref *27*), the rate of energy transfer (k_T) from one donor to a single acceptor is

$$k_T = (k_D + k_{Di})(R_o/R)^6 \quad (11)$$

where R is the distance between the donor and acceptor and R_o is the Förster distance at which the probability of resonance energy transfer equals the sum of the probabilities of all other deactivation pathways. For two acceptors at distances R_1 and R_2 from the donor, the rates of transfer to each acceptor are summed such that

$$k_{T1} + k_{T2} = (k_D + k_{Di})[(R_o/R_1)^6 + (R_o/R_2)^6] \quad (12)$$

Substitution of eq 12 into eq 10 provides

$$E = \frac{R_o^6}{R_o^6 + (R_1^6 R_2^6)/(R_1^6 + R_2^6)} \quad (13)$$

Only when $R_1 = R_2$ does

$$E = \frac{R_o^6}{R_o^6 + R^6/2} \quad (14)$$

In terms of the model in Figure 3, it is possible to calculate the theoretical transfer efficiency, according to eq 13, for any point on the surface of the TyrR molecule defined by the angles θ and ϕ and the distances R_1 and R_2 to a single point (x_o,y_o,z_o) on the DNA. Values of x_o,y_o,z_o, and hence of R_1 and R_2 (eqs 6 and 7), were determined for each donor-labeled position on the DNA, assuming the symmetry of the complex depicted in Figure 3 and the following parameter values: radius of the TyrR monomer, 25 Å; radius of the DNA helix, 5 Å; and translation per nucleotide, 3.3 Å. Such a database of transfer efficiencies was calculated for values of θ and ϕ from 0° to 360° in 10° increments for a given value of R_o. The data sets of transfer efficiencies and θ and ϕ values are presented as three-dimensional surfaces in Figure 4 for four donor-labeled positions on the DNA (−9, −7, −3, and 2). The values of R_o used in these calculations were determined experimentally (see below). Examination of the data sets in Figure 4 indicates that a single transfer efficiency can be given by more than one point on the TyrR surface due to the interplay between the θ and ϕ values and the distances R_1 and R_2. Simulations suggested that determination of transfer efficiencies for three separately labeled donor positions on the DNA would provide sufficient "triangulation" to allow identification of the acceptor site on the TyrR surface. These simulations also indicated that the donor-labeled positions on the oligonucleotide should cover at least one turn of the DNA helix. In the event, four labeled positions were chosen (positions −9, −7, −3, and 2).

RESULTS

Binding of Rhodamine-ATP to TyrR. ATP binds to a single site on TyrR with a half-saturation value of 5−7 μM (*6*). The first task was to determine whether rhodamine-ATP bound to TyrR with a similar affinity so that we could carry out the energy transfer experiment under conditions where the ATP binding site was completely saturated with ligand. This experimental design avoids the need to correct data for the binding of any ATP-free TyrR to the DNA. Initial experiments indicated that the binding of rhodamine-ATP to DNA was not accompanied by any significant change in the fluorescence intensity of the rhodamine-ATP. The

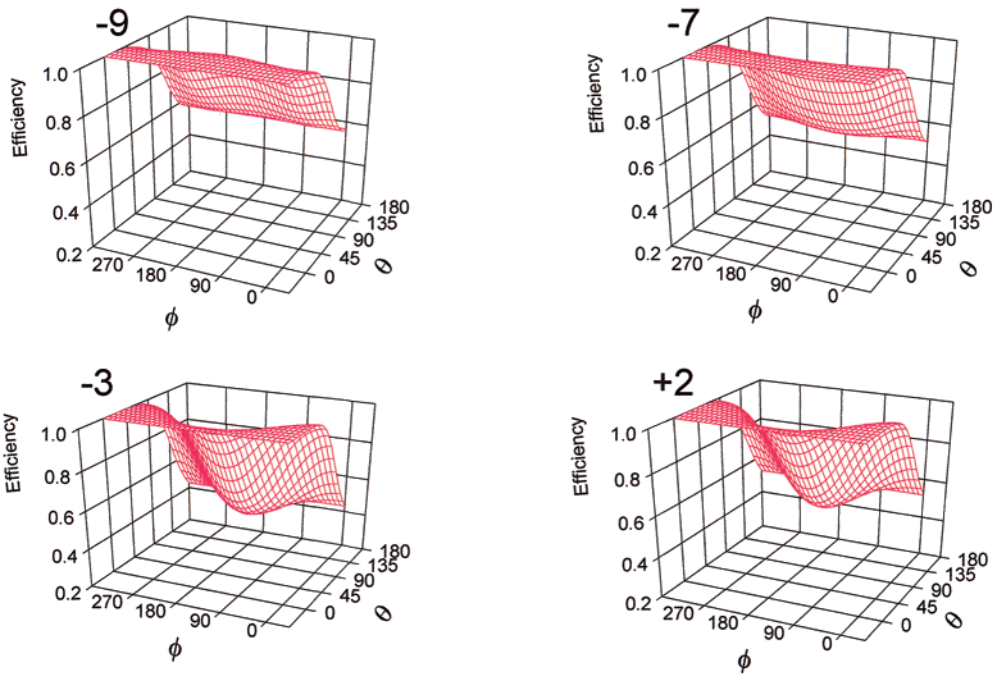

FIGURE 4: Dependence of resonance energy transfer efficiency on θ and ϕ angles that define a point of the surface of the TyrR monomer. The efficiencies are calculated for a donor that is attached at position −9, −7, −3, or 2 on the 30mer oligonucleotide. The transfer distances R_1 and R_2 used to calculate the transfer efficiencies according to eq 13 were determined for the model depicted in Figure 3 (i.e., TyrR radius, 25 Å; DNA helix radius, 5 Å; and translation per nucleotide, 3.3 Å). Note that the distribution of efficiencies is symmetrical about $\phi = 180°$ since we cannot distinguish between a point on the TyrR surface that is behind or in front of the axis of the DNA.

binding was therefore monitored by the increase in the fluorescence anisotropy of rhodamine-ATP on the addition of TyrR, and was assessed at three concentrations of rhodamine-ATP covering 3 orders of magnitude (2, 20, and 200 nM) as shown in Figure 5. Global fitting of the three data sets assuming a 1:1 binding stoichiometry as has been demonstrated for ATP (*6*) provided a value for the dissociation constant of 0.30 μM. Similar titrations under stoichiometric conditions indicated that the 1:1 stoichiometry was maintained when the TyrR existed within the protein−DNA complex.

Binding of TyrR to DNA. Previous studies have shown that the binding of TyrR to fluorescein-labeled DNA either enhances or quenches the quantum yield of the fluorophore depending on the sequence position of the base that is labeled. The reasons for these changes are not fully understood but presumably relate to the way the fluorescence is either quenched or enhanced due to local interactions of the probe with DNA and the TyrR protein, and to the TyrR-induced distortion of the DNA structure (*11*). Thus, the quantum yield of the donor oligonucleotide−fluorescein conjugate varies with the position that is labeled. Because the sixth power of the Förster distance (R_o) is directly proportional to the quantum yield of the donor (eq 4), it was necessary to determine the quantum yield of each of the labeled oligonucleotides under conditions of full saturation with TyrR, but in the absence of the rhodamine-ATP acceptor. This information was then used to determine the value of R_o for each donor−acceptor pair before constructing the database of transfer efficiencies according to eq 13 (Figure 4). The changes in the fluorescence intensity of fluorescein-labeled DNA on the binding of TyrR are shown in Figure 6. Fluorescence was enhanced when the fluorescein was conjugated at positions −9 and 2. There was little change

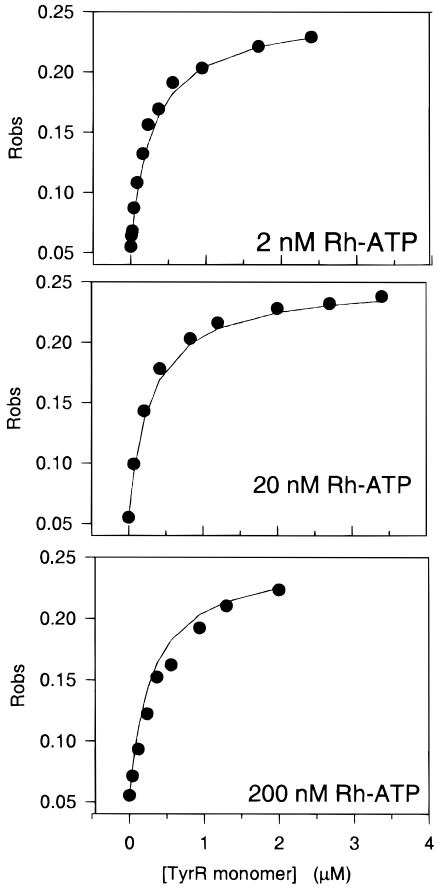

FIGURE 5: Binding of rhodamine-ATP to TyrR determined by steady-state anisotropy titrations at 2, 20, and 200 nM rhodamine-ATP (Rh-ATP). The ordinate scale (R_{obs}) refers to the observed fluorescence anisotropy. The solid line in each panel is the global fit of the three data sets to a single dissociation constant of 300 nM.

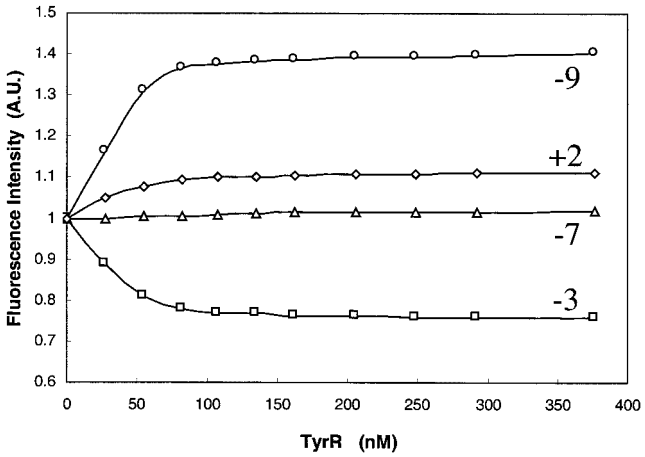

FIGURE 6: Changes in the fluorescence intensity of fluorescein-labeled DNA (50 nM) on binding the TyrR dimer in the presence of 0.2 mM ATPγS. The number for each curve indicates the base position on the DNA 30mer at which the fluorescein is conjugated. Excitation was at 490 nm and emission at 520 nm. The solid lines for the position −9, −3, and 2 conjugates are the nonlinear least-squares fits to the experimental data and provide values for the dissociation constant of 6, 5, and 8 nM, respectively.

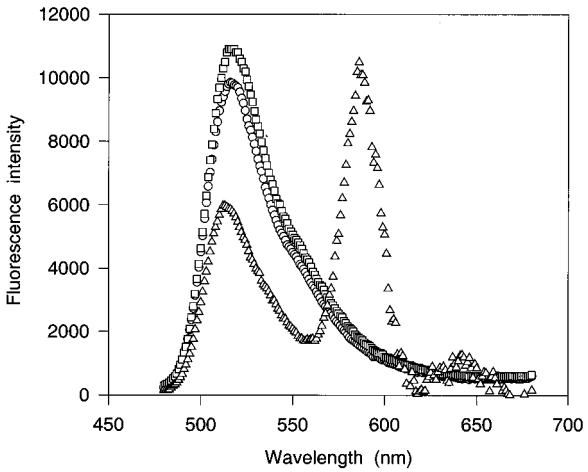

FIGURE 7: Effect of adding TyrR and rhodamine-ATP on the emission spectra of the position 2-labeled oligonucleotide: (○) 50 nM oligonucleotide alone, (□) oligonucleotide in the presence of 1.7 μM tyrR, and (△) oligonucleotide in the presence of 1.7 μM TyrR and 8.36 μM rhodamine-ATP, corrected for the small excitation of the rhodamine label at the excitation wavelength. Excitation was at 465 nm.

Table 1: Characteristics of the Fluorescein-Labeled DNA−TyrR Complex and the FRET Efficiencies on Addition of the Rhodamine-ATP Acceptor

donor position	K_d[a] (nM)	donor quantum yield[b]	R_o (Å)	donor quench[c] (%)	transfer efficiency
−9	6	0.80	56.5	43.8	0.53
−7	−	0.59	53.7	41.4	0.53
−3	5	0.44	51.1	35.3	0.46
2	8	0.64	54.4	36.8	0.52

[a] K_d for the binding of TyrR to DNA in the absence of rhodamine-ATP determined from the titration data depicted in Figure 6. [b] Quantum yield of fluorescein-labeled DNA fully saturated with TyrR but before the addition of the rhodamine-ATP acceptor. [c] Donor quench on addition of the rhodamine-ATP acceptor.

in fluorescence for the position −7 conjugate, but fluorescence was quenched for the position −3 conjugate. Nonlinear least-squares fitting of the titrations for the position −9, −3, and 2 conjugates gave K_d values of 5.9, 4.7, and 8.2 nM, respectively (Table 1). The small change in the fluorescence for the position −7 conjugate precluded its use in determining the binding affinity. The quantum yields determined relative to a fluorescein standard were 0.80, 0.59, 0.44, and 0.64 for the position −9, −7, −3, and 2 conjugates, respectively, providing R_o values of 56.5, 53.7, 51.1, and 54.4 Å, respectively (Table 1). Literature values of R_o for FITC-labeled donors and rhodamine-labeled acceptors are in the range of 40−56 Å (*18*).

Resonance Energy Transfer. Figure 7 shows the emission spectrum of the oligonucleotide (50 nM) labeled at position 2 and is illustrative of the data obtained for the other fluorescein−DNA conjugates. On the addition of 1.7 μM TyrR dimer, the emission is enhanced 10.9%. This compares with the 11.2% enhancement at saturation derived from the titration data for this conjugate in Figure 6. We estimate that under the conditions of the energy transfer experiment more than 95% of the DNA is bound to TyrR, a situation that is favored by the fact that the binding of ATP or ATPγS to TyrR increases the binding affinity of TyrR for DNA by a factor of 4−5 (*11*). Addition of 8.36 μM rhodamine-ATP causes a 36.8% quenching of fluorescein fluorescence, with the concomitant appearance of sensitized rhodamine fluorescence confirming the advent of resonance energy transfer. Similar experiments were carried out for the three other DNA conjugates. The efficiency of energy transfer was determined from the donor quench at a single emission wavelength (515 nm) as well as by measurement of the area under the emission curve. The latter method takes account of the slight apparent blue shift that occurs on the addition of rhodamine-ATP, and was therefore used to compare the experimental values with the theoretical transfer efficiencies. Table 1 lists the transfer efficiencies for the four fluorescein−oligonucleotide−rhodamine-ATP−TyrR complexes. Transfer efficiencies were 0.53, 0.53, 0.46, and 0.52 for the position −9, −7, −3, and 2 conjugates, respectively.

Control experiments indicated that the binding of unlabeled ATP (ATPγS) had no significant effect on the fluorescence intensity of the fluorescein-labeled fluorescein DNA in the TyrR−DNA complex under the conditions of the energy transfer experiment. Nor did rhodamine-ATP have any effect on the fluorescence of the fluorescein-labeled DNA in the absence of TyrR.

Analysis of Transfer Efficiencies. The data sets of θ and ϕ angles and the derived theoretical transfer efficiencies for the four labeled donors are shown in Figure 4. From each data set, a subset of θ and ϕ values was selected which provides theoretical transfer efficiencies that matched the experimentally determined transfer efficiencies listed above and in Table 1. In doing so, we accepted all predicted transfer efficiencies (and their corresponding θ and ϕ angles) that fell within ±2 percentage points of the experimental transfer efficiencies. The exception was 7F30A/30B where predicted efficiencies of 0.56−0.57 were closest to the experimental transfer efficiency of 0.53. The resulting subsets of θ and ϕ angles for the four donor−acceptor pairs are shown in Figure 8. The θ and ϕ angles that satisfied the experimental efficiencies for all four donor−acceptor pairs were identified by plotting θ versus ϕ for the subset of θ and ϕ values shown in Figure 8. This plot of θ versus ϕ for the four donor−

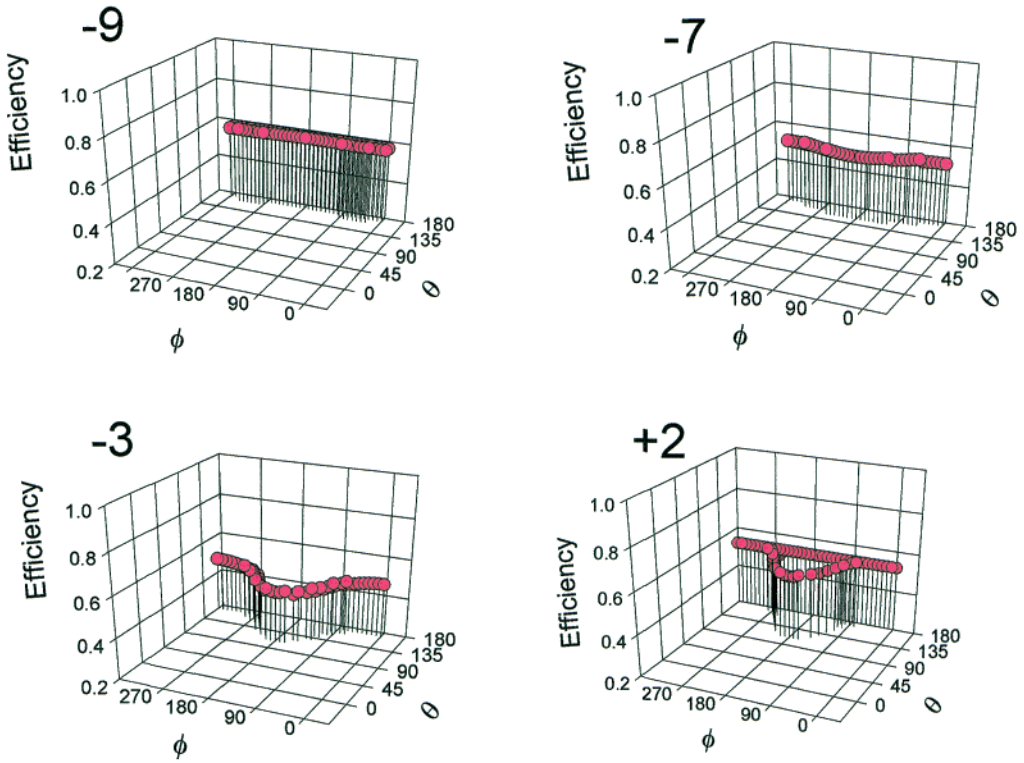

FIGURE 8: θ and ϕ angles of computed transfer efficiencies that fall within ±2 percentage points of the transfer efficiencies determined experimentally for each of the four fluorescein−DNA conjugates. The exception is the position −9-labeled conjugate (top left) where predicted transfer efficiencies of 0.56−0.57 were the closest to the experimental efficiency of 0.53. The number above each panel refers to the position of the label on the oligonucleotide. The θ and ϕ angles were selected from the extensive database depicted in Figure 4 that provided the distances and transfer efficiencies from a donor point on the DNA to any point on the surface of a TyrR monomer (see the text).

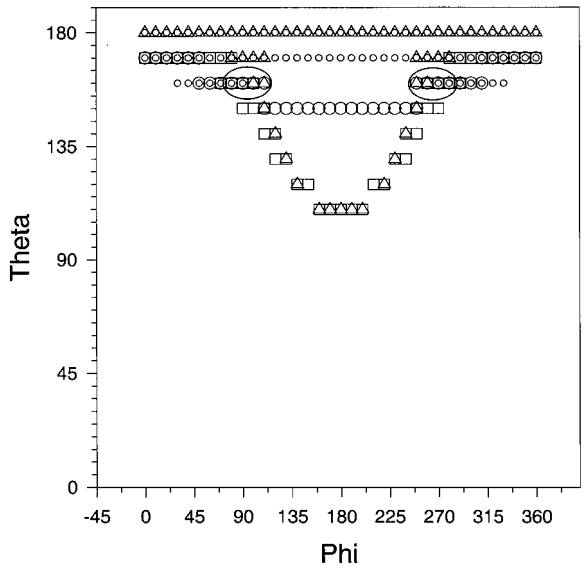

FIGURE 9: Plot of θ vs ϕ for determining those values that match the transfer efficiencies of all four fluorescein−DNA conjugates. The two ovals indicated the region where the experimental transfer efficiencies match those predicted for the model depicted in Figure 3.

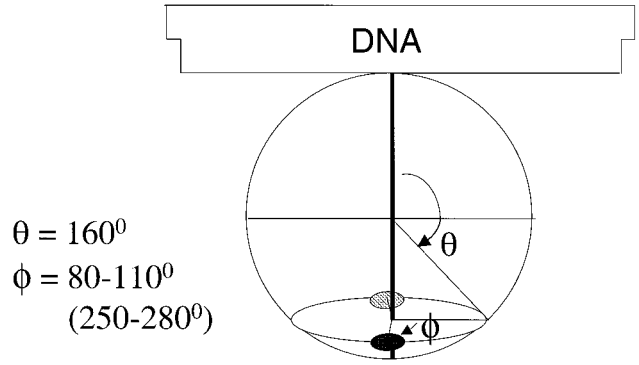

FIGURE 10: Position of the ATP site on TyrR relative to DNA. For clarity, only one monomer of the TyrR dimer is depicted, the second monomer being arranged as shown in Figure 2. The ATP site is at $\theta = 160°$ and at $\theta = 80-110°$ or $\theta = 250-280°$. The two θ positions refer to ATP sites on TyrR that are in front of or behind the axis of the DNA, both positions resulting in equivalent distances from a labeled site on the DNA.

acceptor pairs is presented in Figure 9. As expected, the plot is symmetrical about $\phi = 180°$, since a surface position on a TyrR monomer may be in front of or behind the y plane through the central axis of the DNA, both positions being an equal distance from a labeled position on the DNA. All efficiencies fall within the range of $\theta = 120-180°$, indicating that the ATP binding site is far removed from the DNA interaction site. However, the smallest region where the four data sets overlap (circled area in Figure 9) is given by $\theta = 160°$ and $\phi = 80-110°$ (or 250−280°). At this position, the four experimentally determined transfer efficiencies match those predicted theoretically. The position of this site on the TyrR monomer is shown in Figure 10. The two ϕ positions arise from the fact that it is not possible to determine if the ATP site on the TyrR is in front of or behind the central axis of the DNA, both positions giving rise to the same distances from the fluorescein label on the DNA.

DISCUSSION

Several criteria must be satisfied if fluorescence resonance energy transfer is to be used to measure distances between sites on the *tyrR* DNA and the ATP-binding site on the TyrR protein:

(i) Purified donor-labeled oligonucleotide is required to avoid the need to correct for the presence of unlabeled material.

(ii) The TyrR protein should be fully saturated with the rhodamine-ATP acceptor so that resonance energy transfer can occur in all DNA−TyrR complexes that are formed.

(iii) The DNA should be saturated with TyrR so that every donor on the DNA has the opportunity to transfer energy to the acceptor at the ATP site on TyrR.

(iv) The analysis of the transfer efficiencies must allow for the resonance transfer from one donor on the DNA to two acceptors, one on each of the TyrR monomers.

Requirement (i) was met by separating labeled from unlabeled oligonucleotide by reverse-phase HPLC. Requirements (ii) and (iii) were met by an experimental design that ensured that more than 95% of the ATP sites on TyrR were occupied by rhodamine-ATP and that more than 95% of the DNA sites were occupied by rhodamine-ATP−TyrR. Specific knowledge of the two binding affinities was therefore necessary in planning these experiments. Requirement (iv) was taken into account in the derivation and application of eq 13.

The dissociation constant for the binding of rhodamine-ATP to TyrR was determined directly by the anisotropy titration shown in Figure 5. The value of the dissociation constant (300 nM) is lower than previous estimates for unlabeled ATP (5−7 μM), suggesting that the presence of the rhodamine label may contribute to the binding energy. Greater than 95% saturation of the ATP site with rhodamine-ATP could not be achieved due to the onset of concentration quenching in the fluorometric cuvette. The K_d values for the binding of TyrR to the position −9-, −3-, and 2-labeled conjugates of DNA in the absence of ATP were determined from the quenching/enhancement titrations (Figure 6), and were in the range of 5−8 nM (Table 1). This agrees with the value of 7 nM reported for the binding of TyrR to unlabeled DNA (*11*) determined from competition titrations using labeled and unlabeled DNA. It appears therefore that the labeling of the DNA with fluorescein does not interfere significantly with the binding of TyrR. We note that labeling of the DNA with an aminopropyne extension at position 5 of the uridine resulted in weaker binding [K_d = 425 nM at 20 °C (*11*)] compared to the absence of an effect on the K_d as in the case of the longer extension arm of seven atoms used in the work presented here.

Calculation of the theoretical transfer efficiencies for the model shown in Figure 3 indicated that a single transfer distance between one site on the DNA and the ATP site on TyrR was insufficient to unequivocally locate the ATP site on each monomer of the TyrR dimer. On the other hand, the simulations showed that at least three transfer distances involving three donor-labeled sites on the DNA would be required to determine the position of the ATP site on the TyrR to within narrow limits. The position of the ATP site at θ = 190° and ϕ = 120−130° (or 230−240°) provides theoretical transfer efficiencies that agree with the experimental efficiencies determined for all four donor−acceptor pairs. This places the ATP site approximately 40−45 Å from the nearest point on the DNA and at a point on the TyrR molecule that is far removed from the DNA binding site.

The errors associated with these estimates relate to the assumptions inherent in the model of the DNA−TyrR complex (Figure 3), and assumptions in the application of the Förster theory. The model assumes that the ATP site is on the surface of the TyrR monomer, whereas it is more likely to be buried to some degree in a crevice in the protein structure. This type of error would place the ATP site projected at the protein surface even further removed from the DNA but buried somewhat in the protein structure. The model does not take into account the distance of the fluorescein donor from the helical axis of the DNA nor the effect of binding the TyrR dimer along the major groove compared to the purely linear depiction in Figure 3. The side of the DNA to which TyrR binds is not known, so it is impossible to orient the fluorescein site relative to the TyrR protein. However, an examination of the DNA structure shows that carbon-5 of the uridine, through which the fluorescein is attached by a spacer arm, is in the major groove of the DNA. Thus, if the labeled position is close to the interaction site, as is the case when the label is at position 9, it is likely that the fluorescein moiety is sandwiched between the protein and the DNA and is close to the helical axis of the DNA. If the labeled site is on the side of the DNA opposite the interaction site, the spacer arm would allow the fluorescein group to swing away from the helical axis. Consideration of bond lengths suggests that the length of the spacer arm is about 7.6 Å. On this basis, we estimate that the errors in the transfer distance are no more than ±5%.

The main uncertainty associated with the Förster theory concerns the value of the orientation factor κ^2 (for a review, see ref *18*). We have assumed the dynamic limit ($\kappa^2 = {}^2/_3$). While this is a reasonable assumption for the labeled oligonucleotide in solution, the binding of TyrR causes a significant restriction of the motion of the fluorescein at its point of attachment to the DNA (*16*). Nevertheless, the resulting values of the anisotropy are relatively low [0.025 compared to the zero time anisotropy of 0.35−0.38 (*16*)], indicating considerable motional freedom. The corresponding cone semiangles for the DNA−TyrR dimer complex indicate that the fluorescein label retains considerable motion. The cone semiangles for a fluorescein-labeled 42mer complexed with the TyrR dimer have been determined for positions equivalent to positions −9, −7, and −3 of the 30mer used in the study presented here (*16*). The cone semiangles are 31°, 29°, and 41° for positions −9, −7, and −3, respectively. Stryer (*25*) estimates that the uncertainty in the apparent donor−acceptor distance in assuming $\kappa^2 = {}^2/_3$ is usually less than 20% when the cone angle of the restricted motion of one of the probes is more than 30°. The anisotropy of the rhodamine-ATP bound to the TyrR dimer was also relatively low (0.23). We, therefore, believe that the use of a κ^2 of ${}^2/_3$ is a reasonable approximation.

We conclude that the central domain of TyrR that contains the ATP binding site and possibly a site for the binding of the tyrosine corepressor is far removed from the helix−turn−helix DNA binding domain. Occupation of the ATP site has a 2-fold effect. First, it permits the binding of tyrosine that initiates the self-association of TyrR from a dimer to a

hexamer. Second, it results in a 2−5-fold enhancement of the binding of TyrR to the DNA, an effect that must be transmitted through the TyrR molecule to the C-terminal helix−turn−helix DNA binding domain via a significant allosteric mechanism. Finally, we believe that sufficient triangulation can be achieved by placing a fluorescent probe at several sites within the recognition sequence of the DNA and that the energy transfer approach described here could be of general use in measuring distances between DNA and a single labeled site on the protein.

ACKNOWLEDGMENT

We thank Mathew Dixon for help and advice on the preparation and purification of the TyrR protein and Gerard Marriott, Michael Bailey, and Allen Minton for helpful discussions about the work.

REFERENCES

1. Pittard, A. J., and Davidson, B. E. (1991) *Mol. Microbiol. 5*, 1585−1592.
2. Pittard, A. J. (1996) in *Escherichia coli and Salmonella: Cellular and Molecular Biology* (Neidhardt, F. C., Curtiss, R., Ingraham, J. L., Lin, E. C. C., Low, K. B., Magasanik, B., Reznikoff, W. S., Riley, M., Schaechter, M., and Umbarger, H. E., Eds.) pp 458−484, ASM Press, Washington, DC.
3. Wilson, T. J., Maroudas, P., Howlett, G. J., and Davidson, B. E. (1994) *J. Mol. Biol. 238*, 308−319.
4. Argaet, V. P., Wilson, T. J., and Davidson, B. E. (1994) *J. Biol. Chem. 269*, 5171−5178.
5. Cui, J., and Somerville, R. L. (1993) *J. Biol. Chem. 268*, 5040−5047.
6. Yang, J., Ganesan, S., Sarsero, J., and Pittard, A. J. (1993) *J. Bacteriol. 175*, 1767−1776.
7. Yang, J., Camakaris, H., and Pittard, A. J. (1993) *J. Bacteriol. 175*, 6372−6375.
8. Wilson, T. J., Argaet, V. P., Howlett, G. J., and Davidson, B. E. (1995) *Mol. Microbiol. 17*, 483−492.
9. Walker, J. E., Saraste, M., Runswick, M. J., and Gay, N. J. (1982) *EMBO J. 8*, 945−951.
10. Henijoff, S., and Wallace, J. C. (1988) *Nucleic Acids Res. 16*, 6191−6204.
11. Morett, E., and Segovia, L. (1993) *J. Bacteriol. 175*, 6067−6074.
12. Kwok, T., Yang, J., Pittard, A. J., Wilson, T. J., and Davidson, B. E. (1995) *Mol. Microbiol. 17*, 471−481.
13. Bailey, M. F., Davidson, B. E., Haralambidis, J., Kwok, T., and Sawyer, W. H. (1998) *Biochemistry 37*, 7431−7443.
14. Andrews, A. E., Lawley, B., and Pittard, A. J. (1991) *J. Bacteriol. 173*, 5068−5078.
15. Andrews, A. E., Dickson, B., Lawley, B., Cobbett, C., and Pittard, A. J. (1991) *J. Bacteriol. 173*, 5079−5085.
16. Hwang, J. S., Yang, J., and Pittard, A. J. (1997) *J. Bacteriol. 179*, 1051−1058.
17. Hwang, J. S., Yang, J., and Pittard, A. J. (1999) *J. Bacteriol. 181*, 6411−6418.
18. Bailey, M. F., Hagmar, P., Millar, D. P., Davidson, B. E., Tong, G., and Haralambidis, J. (1995) *Biochemistry 34*, 15802−15812.
19. Clegg, R. M. (1992) *Methods Enzymol. 211*, 353−388.
20. Van der Meer, B. W., Coker, G., and Chen, S.-Y. (1994) *Resonance Energy Transfer. Theory and Data*, VCH, New York.
21. Heyduk, T., and Lee, J. C. (1992) *Biochemistry 31*, 5165−5171.
22. Furey, W. S., Joyce, C. M., Osborne, M. A., Klenerman, D., Peliska, J. A., and Balasubramanian, S. (1998) *Biochemistry 37*, 2979−2990.
23. Jameson, D. M., and Eccleston, J. F. (1997) *Methods Enzymol. 278*, 363−390.
24. Hagmar, P., Bailey, M., Tong, G., Haralambidis, J., Sawyer, W. H., and Davidson, B. E. (1995) *Biochim. Biophys. Acta 1244*, 259−268.
25. Corrie, J. E. T., Eccleston, J. F., Danter, Z., Moore, M. H., and Turkenbery, J. P. (1998) *Biophys. J. 74*, A180.
26. Weber, G., and Teale, F. W. J. (1956) *Trans. Faraday Soc. 53*, 646−655.
27. Stryer, L. (1978) *Annu. Rev. Biochem. 47*, 819−846.

BI0000723